

Medial Axis Approximation with Bounded Error

Svetlana Stolpner
 School of Computer Science
 McGill University
 Montréal, Québec, Canada
 sveta@cim.mcgill.ca

Sue Whitesides
 Department of Computer Science
 University of Victoria
 Victoria, British Columbia, Canada
 sue@uvic.ca

Abstract—A common approach to approximating the medial axis decides the presence of medial points in a region of non-zero size by analyzing the gradient of the distance transform at a finite number of locations in this region. In general, algorithms of this type do not guarantee completeness. In this paper, we consider a novel medial axis approximation algorithm of this type and present an analysis in the 2D case that reveals the geometric relationship between the quality of the medial axis approximation and the number and distribution of samples of the gradient of the distance transform. We use an extension of this algorithm to 3D to compute qualitatively accurate medial axes of polyhedra, as well as Voronoi diagrams of lines. Our results suggest that medial axis approximation algorithms based on sampling of the distance transform are theoretically well-motivated.

Keywords—medial axis approximation; Voronoi diagram approximation; distance field method

I. INTRODUCTION

Let \mathcal{B} be a subset of \mathbb{R}^2 or \mathbb{R}^3 . Then the *medial axis* M of \mathcal{B} is the locus of the set of points that have at least two closest points on \mathcal{B} , and further satisfy the property that if p lies on the medial axis and its closest points on \mathcal{B} are distance d from p , then the interior of the *medial ball* at p of radius d has an empty intersection with \mathcal{B} . Figure 1 shows a 2D and a 3D shape, together with their medial axes, computed using a variant of the method described in this paper. Generically, the medial axis M of \mathcal{B} has one less dimension than the space in which \mathcal{B} lies. When \mathcal{B} forms the boundary of an interior region, the union of the complete set of medial balls interior to \mathcal{B} reconstructs completely the shape bounded by \mathcal{B} .

The medial axis is the continuous counterpart of the Voronoi diagram. The vertices of the Voronoi diagram of a set S of points sampled on \mathcal{B} have been used to generate approximations of the medial axis of \mathcal{B} [1], [2]. The medial axis of a polygon is a subset of the edges of the Voronoi diagram of the polygon; namely, bisectors of polygon edges and their incident polygon vertices are not part of the medial axis [3]. For sets of disjoint convex objects, such as lines and points, the medial axis and Voronoi diagram are equivalent.

The medial axis is a very useful shape descriptor as it captures notions of local thickness (given by the radius of the medial balls, see Figure 1(Top)), part-structure and

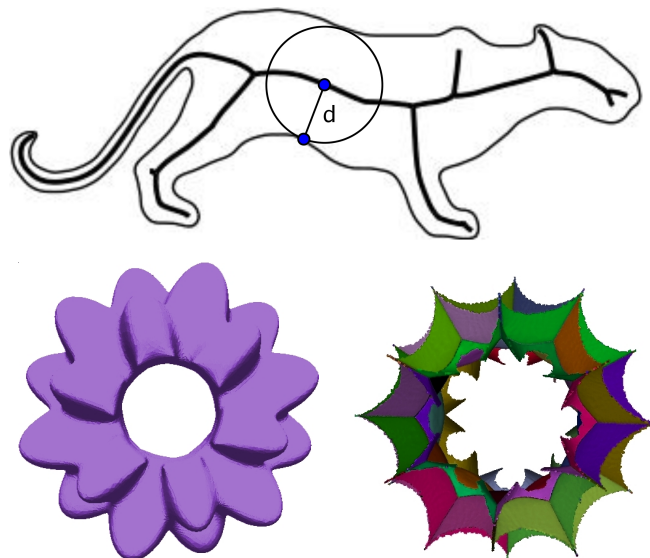


Figure 1. Top: The medial axis of a 2D shape, with a medial ball of radius d overlaid (Adapted from [9]). Bottom: A 3D shape and its medial axis.

symmetry of an object [4]. It has been used in a variety of different applications, such as character animation [5], virtual endoscopy [6] and shape matching [7]. A survey of recent mathematical advances, algorithms and applications can be found in [8].

The following notion in \mathbb{R}^2 (similarly for \mathbb{R}^3) will be key. The *Euclidean distance transform* of $\mathcal{B} \subset \mathbb{R}^2$ is given by $D(p) = -\inf_{q \in \mathcal{B}} d(p, q)$, where $d(p, q)$ denotes Euclidean distance. Then $\nabla D : \mathbb{R}^2 \rightarrow \mathbb{R}^2$ is a vector field that assigns each point in the plane the direction to its closest point on \mathcal{B} . ∇D is a smooth vector field on $\mathbb{R}^2 \setminus M \setminus \mathcal{B}$. For a point p on the medial axis of \mathcal{B} , $\nabla D(p)$ is multi-valued.

As we will review in the next section, there is substantial interest in designing algorithms that provide qualitatively good approximations of the medial axis. Many of these algorithms, which we call *distance field methods*, sample ∇D values to determine whether the medial axis passes inside a given spatial region. However, such methods typically do not guarantee completeness; some medial axis points may be missed. Often, quality of the approximation is assessed

subjectively by visual inspection. Furthermore, notions of quality differ depending on the application.

Goals and Contributions of this work: Our goal is to initiate, for distance field methods, a study of the quality of the medial axis approximation as a function of the number N of ∇D samples and how they are chosen. In particular, based on tools for identifying medial points by distance field methods developed in Section III, we present algorithm DECIDEMA2D for approximating the medial axis of a 2D shape in Section IV. We analyze the 2D case in Section V to obtain a geometric description of the missed medial points. Based on this analysis, we define a notion of quality, which as discussed in Section VI is consistent with current practice. Further, we use DECIDEMA2D to design algorithm APPROXMA2D for medial axis approximation in Section VI that is able to give the user a geometric description of the missed medial points. We extend the algorithm to 3D (where many of the applications lie) and show some experimental results in Section VII. The visual quality of the 3D experimental results suggests that it is possible to design a 3D algorithm that provably detects a dense sampling of significant medial points.

II. PREVIOUS WORK

We will consider classes of algorithms for the exact and approximate computation of the medial axis in 2 and 3 dimensions.

A. Exact Methods

The medial axis of a polygon consists of straight sections and parabolic arcs. For simple polygons, there exists a linear-time algorithm for medial axis construction [3]. The medial axis of a polyhedron is a collection of quadric surfaces intersecting along edges of higher algebraic degree. Therefore, it is a complicated object and is difficult (and often unnecessary) to compute exactly. When this is desired, [10] use exact arithmetic to compute the edges of the medial axis of polyhedra having a small number of faces.

B. Voronoi Methods

For objects in 2D and 3D approximated using a set of points sampled on their boundary, Voronoi-based methods approximate the medial axis with a subset of the Voronoi vertices and edges of the boundary points. Of these, [1] and [2] prove convergence of a subcomplex of the Voronoi diagram of the set of points sampled on the boundary of an object to the medial axis of the object as the sampling density approaches infinity. However, for a finite sampling rate, the density of medial points computed varies within the object depending on the object shape, which may not be desirable for certain applications. Distance field methods, described below, are able to output medial points with a user-defined density. Figure 2 illustrates the difference in outputs for a Voronoi-based method and our distance field method.



Figure 2. Medial points computed with the Power Crust [1] (Centre) and the set of medial points found with our distance field method (Right) for a polyhedron with 2,838 vertices, where the vertices are used as input to the Power Crust. Note that the medial points on the left are very sparse in the navel and pelvic areas (concavities).

C. Distance Field Methods

This type of algorithms consider the nearest boundary elements to a finite number of query points. Space is decomposed into possibly overlapping cells and the goal is to find those cells that are intersected by the medial axis. Vleugels and Overmars [11] use spatial subdivision to approximate the generalized Voronoi diagram of a set of disjoint convex polytopes in any dimension by considering the nearest boundary elements to cell vertices. Etzion and Rappaport [12] perform recursive spatial subdivision until each cell contains one vertex of the generalized Voronoi diagram of a polyhedron. Foskey et al. [13] approximate the medial axis of a polyhedron with axis-aligned facets, with computations accelerated by graphics hardware. Finally, a continuous measure of average outward flux of the gradient of the distance transform in a region shrinking to a point has been shown to be indicative of the presence of the medial axis at that point. When flux is approximated by a sum of directions to nearest boundary locations to points sampled on the boundary of a cell, [9] describes an algorithm to compute locations of the 2D medial axis, while [14] describes a coarse-to-fine algorithm to find cells intersected by the medial axis of a polyhedron.

In general, algorithms of this type, in particular the work cited above, do not guarantee completeness, *i.e.*, there may be cells that are intersected by the medial axis that are not found by the algorithm. Furthermore, in general, research in this area has not provided analysis of the quality of the approximation as a function of the number of query points considered. Our contribution shows how such an analysis can be done as a step toward giving these approaches a more scientific basis.

III. TOOLS FOR IDENTIFICATION OF MEDIAL POINTS

This section provides the basis for the design of our algorithm in Section IV.

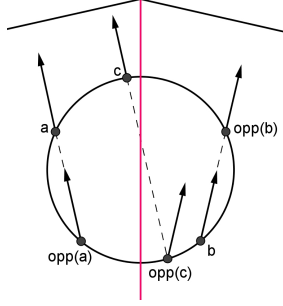


Figure 3. $\nabla D(a) = \nabla D(\text{opp}(a))$ and $\nabla D(b) = \nabla D(\text{opp}(b))$, while $\nabla D(c) \neq \nabla D(\text{opp}(c))$.

Let $\mathcal{B} \subset \mathbb{R}^2$. Let \mathcal{M} be the medial axis of \mathcal{B} . Let C be the boundary of a circle that has an empty intersection with \mathcal{B} .

Let $l(a, b)$ be a line through a and b . For $a \in C$, we shall define the *opposite* of a , $\text{opp}(a)$, as follows. If $l(a, a + \nabla D(a))$ is tangent to C , then $\text{opp}(a) = a$. Otherwise, $\text{opp}(a)$ is the other point of intersection of $l(a, a + \nabla D(a))$ with C besides a . Figure 3 shows some examples of points and their opposites.

Let (a, b) denote the closed line segment with endpoints a and b . Let $d(a, b)$ denote the length of (a, b) .

Lemma 1: Consider two points a and $b = a + \gamma \cdot \nabla D(a)$, for γ a scalar. If e is the unique closest point on \mathcal{B} to a and also to b , then e is the unique closest point on \mathcal{B} for any point $c \in (a, b)$.

Proof: Suppose there exists a point d on \mathcal{B} such that $d \neq e$ and

$$d(c, d) \leq d(c, e). \quad (1)$$

As e is the unique closest point to b ,

$$d(b, d) > d(b, e). \quad (2)$$

By the triangle inequality,

$$\begin{aligned} d(b, d) &\leq d(b, c) + d(c, d) \\ &\leq d(b, c) + d(c, e) \\ &= d(b, e), \end{aligned}$$

where the second inequality follows from (1) and the last by collinearity of b, c, e . Therefore, $d(b, d) \leq d(b, e)$, contradicting (2). ■

Corollary 2: If $b = a + \gamma \cdot \nabla D(a)$ for a scalar γ and $\nabla D(a) = \nabla D(b)$, then no point of the medial axis lies on (a, b) .

In particular, this holds for $b = \text{opp}(a)$ (see Figure 3).

Corollary 3: Let $b = a + \gamma \cdot \nabla D(a)$ and $d = c + \delta \cdot \nabla D(c)$, where $\gamma, \delta \in \mathbb{R}$ and $a, c \in C$. If $\nabla D(a) = \nabla D(b)$ and $\nabla D(c) = \nabla D(d)$, then (a, b) and (c, d) do not cross.

Proof: Suppose $(a, \text{opp}(a))$ and $(b, \text{opp}(b))$ cross at a point c . Then ∇D is multi-valued at c . But by Lemma 1, ∇D only has one value along $(a, \text{opp}(a))$ and $(b, \text{opp}(b))$. ■

Lemma 4: Consider two points a and $b = a + \gamma \cdot \nabla D(a)$, such that (a, b) does not intersect \mathcal{B} and γ is a non-zero scalar. If no medial points lie on (a, b) , then $\nabla D(a) = \nabla D(b)$.

Proof: Suppose that γ is positive. For a contradiction, let A be the unique closest point to a on \mathcal{B} , let B be the unique closest point to b on \mathcal{B} , $A \neq B$. Then

$$d(b, B) < d(b, A) \quad (3)$$

and

$$d(a, A) < d(a, B). \quad (4)$$

Then

$$\begin{aligned} d(a, B) &\leq d(a, b) + d(b, B) \\ &< d(a, b) + d(b, A) \\ &= d(a, A), \end{aligned}$$

where the second inequality follows by (3) and the last by collinearity. Therefore, $d(a, B) < d(a, A)$, contradicting (4). Therefore, $A = B$ and $\nabla D(a) = \nabla D(b)$, regardless of whether a medial point lies on (a, b) .

Now suppose that γ is negative and no medial points lie on (a, b) . To complete the proof, we use some tools from the theory of geometric curve evolution. The medial axis M is the set of shocks of the grassfire flow applied to $\mathbb{R}^2 \setminus \mathcal{B}$, as explained in [4]. The grassfire flow evolves a moving front $W(t)$ according to the equation $\frac{\partial W}{\partial t} = \mathbf{n}$, where \mathbf{n} is the unit normal to W with the initial condition $W(0) = \mathcal{B}$. For all points $p \in \mathbb{R}^2 \setminus M \setminus \mathcal{B}$, \mathbf{n} is given by $-\nabla D(p)$. Suppose $W(t_0)$ passes through a . Since (a, b) contains no medial points, point a on $W(t_0)$ after time γ becomes point $b = a + \gamma \nabla D(a)$ on $W(t_0 - \gamma)$. The normal to $W(t_0 - \gamma)$ at b is $\nabla D(a)$, a known property of the grassfire flow [15]. On the other hand, the normal to $W(t_0 - \gamma)$ at b is $\nabla D(b)$. Therefore, $\nabla D(a) = \nabla D(b)$. ■

Corollary 5: If $b = a + \gamma \cdot \nabla D(a)$, where $\gamma \in \mathbb{R}$, if (a, b) does not intersect \mathcal{B} and if $\nabla D(a) \neq \nabla D(b)$, then there is a medial point in (a, b) .

Corollary 5 will serve as the basis for the algorithm for medial point detection described in the next section, as will the following 2 lemmas.

From now on, we use the expression of 2 vectors $\nabla D(p)$ and $\nabla D(q)$ being to the “same side” of the line through p and q , $l(p, q)$, in the following way. Vector $\nabla D(p)$ and $\nabla D(q)$ are to the same side of $l(p, q)$ whenever $\text{sgn}(\nabla D(p) \cdot \mathbf{n}(p, q)) = \text{sgn}(\nabla D(q) \cdot \mathbf{n}(p, q))$, where $\mathbf{n}(p, q)$ is a vector normal to $l(p, q)$.

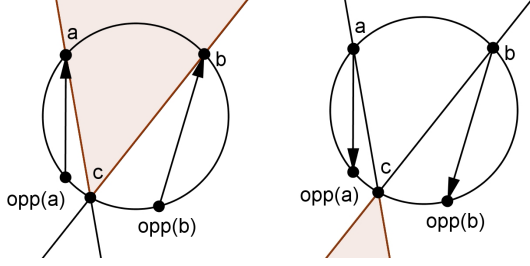


Figure 4. Cases A (Left) and B (Right) of Lemma 8.

Lemma 6: Suppose a and b are two points on C , $b \neq opp(a)$, and there are no medial points along (a, b) . Then $\nabla D(a)$ and $\nabla D(b)$ are to the same side of $l(a, b)$.

Proof: Suppose that there are no medial points along (a, b) , yet $\nabla D(a)$ and $\nabla D(b)$ are to different sides of $l(a, b)$. Since there are no medial points along (a, b) , then ∇D varies smoothly for points along (a, b) . Thus, at some point c , $\nabla D(c)$ is aligned with (a, b) . Since there is no medial point along (a, b) , by Corollary 5, either $\nabla D(a) = \nabla D(c)$ or $\nabla D(b) = \nabla D(c)$. Then $b = opp(a)$, a contradiction. ■

Corollary 7: If $\nabla D(a)$ and $\nabla D(b)$ are to different sides of $l(a, b)$, then there is a medial point on (a, b) .

For a circle C that has an empty intersection with \mathcal{B} , let Φ be a set of N points sampled on C , such that the maximum distance between neighbouring points in Φ is small. Let $\Psi = \{opp(\phi_i), \phi_i \in \Phi\}$. Let $\Theta = \Phi \cup \Psi$. For two points a and b in Θ , let $\widehat{(a, b)}$ denote the closed arc of C connecting a and b , where the choice of arc is that empty of other points in Θ , unless otherwise specified.

Lemma 8: Let a and b be a pair of nearest neighbours in Θ , such that $\nabla D(a)$ and $\nabla D(b)$ are to the same side of $l(a, b)$. Suppose that there exists a point $c \in \Theta, c \neq opp(a), opp(b)$ in $\widehat{(opp(a), opp(b))}$ (where the choice of arc is that not containing a or b). Then there is a medial point in C on (a, c) or (b, c) .

Proof: Suppose that there is no medial point inside C . Consider (a, c) and (c, b) . Since there is no medial point inside C , by Lemma 6, $\nabla D(c)$ is to the same side of $l(a, c)$ as $\nabla D(a)$ and also to the same side of $l(b, c)$ as $\nabla D(b)$. By Corollary 3, $(a, opp(a))$ and $(b, opp(b))$ do not cross.

For the remainder of the proof, we orient (a, b) horizontally, such that a is to the left of b , as in Figure 4. The next two paragraphs handle the two cases: (A) $\nabla D(a)$ and $\nabla D(b)$ both point above $l(a, b)$ and (B) $\nabla D(a)$ and $\nabla D(b)$ both point below $l(a, b)$.

If $\nabla D(a)$ and $\nabla D(b)$ both point above $l(a, b)$, then $\nabla D(a)$ is to the right of $\widehat{(a, c)}$ and $\nabla D(b)$ is to the left of (b, c) because $c \in (opp(a), opp(b))$. Then $\nabla D(c)$ is to the right of $l(a, c)$ and to the left of $l(b, c)$. Thus $opp(c) \in \widehat{(a, b)}$, an impossibility since a and b are nearest neighbours in Θ and $opp(a) \neq c$ and $opp(b) \neq c$. Refer to Figure 4 (Right).

If $\nabla D(a)$ and $\nabla D(b)$ are both below the line through (a, b) , then $\nabla D(a)$ is to the left of $l(a, c)$ and $\nabla D(b)$ is to the right of $l(b, c)$. Then $\nabla D(c)$ is to the left of the line through (a, c) and to the right of the line through (b, c) . Thus $opp(c)$ is again in $\widehat{(a, b)}$, an impossibility as we argued above. Refer to Figure 4 (Left).

Therefore, if there exists a point $c \in \Theta$ in the arc $\widehat{(opp(a), opp(b))}$, then there is a medial point in C . In particular, there is a medial point on (a, c) or (b, c) . ■

Algorithm 1 DECIDEMA2D(\mathcal{B}, C, Φ)

Require: Boundary \mathcal{B} , circle C not intersecting \mathcal{B} , set of points Φ distributed on C .

Ensure: ‘True’ if C contains a medial point, ‘Undetermined’ if no such conclusion can be drawn.

```

1: for all  $\phi_i \in \Phi$  do
2:   if  $\nabla D(\phi_i) \neq \nabla D(opp(\phi_i))$  then
3:     Return ‘True’
4:   end if
5: end for
6: Let  $\Theta = \Phi \cup \{opp(\phi_i) | \phi_i \in \Phi\}$ 
7: for all pairs of nearest neighbours  $\theta_i$  and  $\theta_j$  in  $\Theta$  do
8:   if  $\nabla D(\theta_i)$  and  $\nabla D(\theta_j)$  are to different sides of
    $l(\theta_i, \theta_j)$  then
9:     Return ‘True’
10:  end if
11: end for
12: for all pairs of nearest neighbours  $\theta_i$  and  $\theta_j$  in  $\Theta$  do
13:   if  $\widehat{(opp(\theta_i), opp(\theta_j))}$  contains points in  $\Theta$  then
14:     Return ‘True’
15:   end if
16: end for
17: Return ‘Undetermined’
```

IV. ALGORITHM

We propose the following algorithm for the detection of regions of 2D space that contain medial axis points.

Lemma 9: If DECIDEMA2D(\mathcal{B}, C, Φ) returns ‘True’ then C contains a medial point.

Proof: If DECIDEMA2D returns ‘True’ on line 3, then by Corollary 5, there is a medial point in C . If DECIDEMA2D returns ‘True’ on line 8, then by Corollary 7, there is a medial point in C . If DECIDEMA2D returns ‘True’ on line 13, then by Lemma 8, there is a medial point in C . ■

Algorithm DECIDEMA2D performs $O(N)$ distance queries and additionally takes $O(N \log N)$ time to find nearest neighbours in Θ .

V. MISSING A MEDIAL POINT

In this section, we consider the possibility that DECIDEMA2D(\mathcal{B}, C, Φ) returns ‘Undetermined’, yet the convex hull of $\Theta = \Phi \cup \{opp(\phi_i) | \phi_i \in \Phi\}$ contains a medial

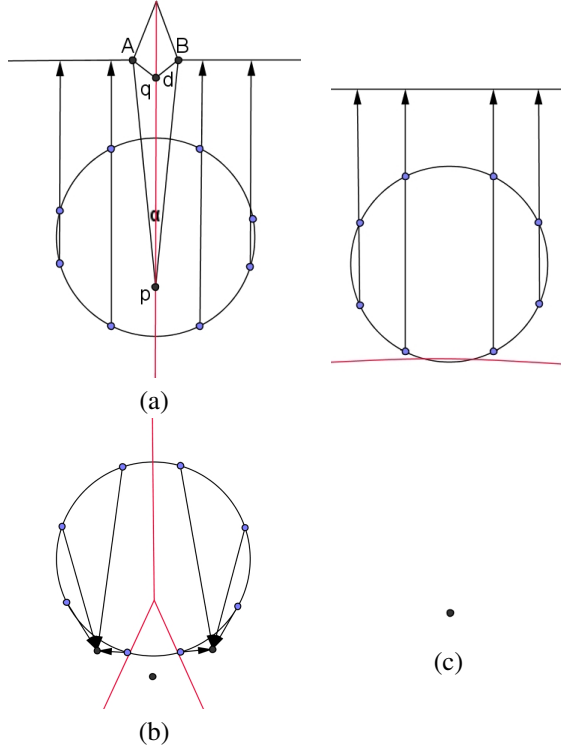


Figure 5. Situations when Algorithm 1 returns ‘Undetermined’ while a section of the medial axis passes through circle C .

point p . Some situations when this happens are illustrated in Figure 5.

Although our algorithm fails to identify medial points in these examples, in this section we will show that whenever circle C contains a medial point p and DECIDEMA2D returns ‘Undetermined’, when sample points on C are distributed appropriately, either (1) p has a small object angle, (2) p is close to \mathcal{B} , (3) C is close to \mathcal{B} , or (4) the medial point p is shallow inside C . The medial points p and q in Figure 5 are equidistant from points A and B on \mathcal{B} . Point p has a small object angle $\angle ApB$, while point q is close to \mathcal{B} . Figure 5(b) shows an example of C being close to \mathcal{B} , while Figure 5(c) shows an example of missing medial points that are shallow inside C .

Suppose that a medial axis point p is on or inside the convex hull of Θ . Point p is equidistant from two locations on \mathcal{B} ; let us call these locations A and B . Let a be the point of intersection of (p, A) with C ; define b similarly for B . Points a and b cannot be in Θ , because DECIDEMA2D ensured that $\nabla D(a) = \nabla D(\text{opp}(a))$ and $\nabla D(b) = \nabla D(\text{opp}(b))$, and by Corollary 2, $(a, \text{opp}(a))$ and $(b, \text{opp}(b))$ do not contain medial points. Call the two nearest neighbours of a in Θ x and y ; similarly, the nearest neighbours of b in Θ are x' and y' . Also, since DECIDEMA2D returned ‘True’, $\nabla D(x)$ and $\nabla D(y)$ are to the same side of $l(x, y)$ and $\nabla D(x')$ and

$\nabla D(y')$ are to the same side of $l(x', y')$.

For a medial axis point p inside the convex hull of Θ , we consider two cases:

- Case 1: $\nabla D(a)$ is to the same side of $l(x, y)$ as are $\nabla D(x)$ and $\nabla D(y)$ and also $\nabla D(b)$ is to the same side of $l(x', y')$ as are $\nabla D(x')$ and $\nabla D(y')$.
- Case 2: Either $\nabla D(a)$ is to the other side of $l(x, y)$ as $\nabla D(x)$ and $\nabla D(y)$ or $\nabla D(b)$ is to the other side of $l(x', y')$ as $\nabla D(x')$ and $\nabla D(y')$.

Let L be the longest length of the shortest arc on C between two neighbouring points sampled on C . We require that L decreases as N increases. Let R be the radius of C . Let N be big enough such that $L < 2R$. Let $d = d(p, A) = d(p, B)$. We will study the nature of the medial points missed as a function of L , R and d .

A. Case 1

Suppose that C contains a medial point p as described by Case 1, yet DECIDEMA2D(\mathcal{B}, C, Φ) returned ‘Undetermined’.

We first show that, in this case, $b \in \widehat{(x, y)}$. Suppose $b \notin \widehat{(x, y)}$. Note that $(x, \text{opp}(x))$ and $(y, \text{opp}(y))$ do not cross, by Corollary 3. Let $(x, \text{opp}(x))$ be the arc of C not containing y and $(y, \text{opp}(y))$ be the arc of C not containing x . Point b cannot be in $(x, \text{opp}(x))$ or $(y, \text{opp}(y))$ because $(x, \text{opp}(x))$ and $(y, \text{opp}(y))$ cannot cross (p, b) , by Corollary 3. Thus $b \in (\text{opp}(x), \text{opp}(y))$. Consider x' and y' . Since algorithm DECIDEMA2D returned ‘Undetermined’, $(\text{opp}(x), \text{opp}(y))$ does not contain any points of Θ in its interior. Therefore, x' and y' are $\text{opp}(x)$ and $\text{opp}(y)$. Vectors $\nabla D(x)$ and $\nabla D(y)$ point to the same side of $l(x, y)$ as $\nabla D(a)$, that is, outside of C . Likewise, $\nabla D(x')$ and $\nabla D(y')$ point to the same side of $l(x', y')$ as $\nabla D(b)$, that is, outside of C . Thus, $\nabla D(x) = \nabla D(\text{opp}(x)) = x - \text{opp}(x)$. Since one of $\nabla D(x')$ or $\nabla D(y')$ is $D(\text{opp}(x))$, one of $\nabla D(x')$ or $\nabla D(y')$ points to a different side of (x', y') as does $\nabla D(b)$. Since we are in Case 1, point $b \notin (\text{opp}(x), \text{opp}(y))$. It must lie in $\widehat{(x, y)}$.

Suppose that (x, y) is aligned with the horizontal and that x is left of y . Call $d(p, A)$ the distance d from the medial axis point p to the boundary \mathcal{B} . Call the angle between (p, A) and (p, B) the object angle α of the medial point p . Let R be the radius of C . Let X be the nearest point on \mathcal{B} to x and Y be the nearest point of \mathcal{B} to y . We will show that if the missed medial point p is of the type in Case 1, then either the distance or the object angle is bounded in terms of R and L .

Let $d(p, A) = d(p, B)$ be d . When $d < 2L$, arguably, this is a good bound on the quality of the medial point missed.

When $d \geq 2L$, we look for an upper bound on the object angle α given L , R and d . Consider the isosceles triangle with vertices p , A and B . We know that a and b are in $\widehat{(x, y)}$. We now argue that $\triangle pAB$ must be fully contained in the region right of $l(x, \text{opp}(x))$ and left of $l(y, \text{opp}(y))$.

Suppose that A lies outside this region, left of $l(x, opp(x))$. Then, since (x, X) and (p, A) do not cross by Corollary 3, X is closer to p than is A , contradicting the fact that A is a closest point on B to p .

For an upper bound on α , let us consider an isosceles triangle $\triangle u w v$ such that $d(u, w) = d(w, v) = d$ and such that $\triangle u w v$ is fully contained inside the region right of $l(x, opp(x))$ and left of $l(y, opp(y))$. We look for a placement of vertex w on or inside the convex hull of Θ such that $\angle u w v$ is maximum. The maximum $\angle u w v$ is achieved when $opp(x)$ and $opp(y)$ coincide at a point z on C . The region right of $l(x, z)$ and left of $l(y, z)$ is a wedge $x z y$. For an upper bound on α , let the length of arc (x, y) be L . The inscribed acute angle ϕ made by the chord (x, y) with z is $\arcsin(L/2R)$ (see Figure 6).

Consider all possible isosceles triangles $u w v$ that lie inside the wedge $x z y$, such that $d > L$. We want to find the position of this triangle that gives the maximum $\angle u w v$. Suppose that $\angle u w v$ is maximum when w lies strictly inside the convex hull of Θ (see Figure 6(a)). Since $\angle u w v$ is maximum and $d > L$, each of u and v lies on one of $l(z, x)$ and $l(z, y)$. Suppose that u lies on $l(z, x)$. Now consider translating the triangle $u w v$ in the direction parallel to (z, x) , so that u moves along $l(z, x)$ until w lies on the chord (x, y) instead of inside the convex hull. Since $\phi > 0$, v no longer lies on $l(z, y)$ and, since $d \geq 2L > d(x, y)$, $\angle u w v$ can be increased so that v lies on $l(z, y)$ (see Figure 6(b)). Thus, $\angle u w v$ is not maximum when w lies strictly inside the convex hull of Θ . Therefore, to maximize $\angle u w v$, let us place w on the chord (x, y) of C .

We know that the maximum value of $\angle u w v$ occurs when w lies on the chord (x, y) . Now we want to know an upper bound on $\angle u w v$ when w lies on the chord (x, y) . We measure the height of w with respect to z as follows. Let x^* and y^* be the intersections of a line through w with $l(x, z)$, $l(y, z)$, such that $\angle z x^* y^* = \angle z y^* x^*$. Then $d(x^*, z) = d(y^*, z) = h$ is the height of w in the wedge $x y z$ (see Figure 6(c)).

For all possible points z on C , either $h \leq d(z, y)$ or $h \leq d(z, x)$. Suppose it is the latter. Since (x, z) and (y, z) are chords of C , $d(x, z) \leq 2R$ and $d(y, z) \leq 2R$. Since $d(z, y) \leq 2R$, $h \leq 2R$. Consider an isosceles triangle $\triangle x' z y'$ such that $d(z, x') = d(z, y') = 2R$ and $\angle x' z y' = \phi$. Call $d(x', y')$ L' . The triangle $u w v$ lies inside the wedge $x' z y'$. Then $h = d(x^*, z) = d(y^*, z) \leq 2R$. That is, w lies on or below (x', y') in the wedge $x' z y'$. By earlier arguments, w can be placed on (x', y') (see Figure 6(c)). Since $L < 2R$, then necessarily $d(x', y') < \sqrt{2}L$. Again, by earlier arguments, $\angle u w v$ can be increased by placing u on $l(x, z)$ and v on $l(y, z)$ (see Figure 6(d)).

We want to find the position of w on (x', y') such that $\triangle u w v$ is inside the wedge $x' z y'$ that maximizes $\angle u w v$, where

$$\angle u w v = \phi + \angle x' u w + \angle w v y'.$$

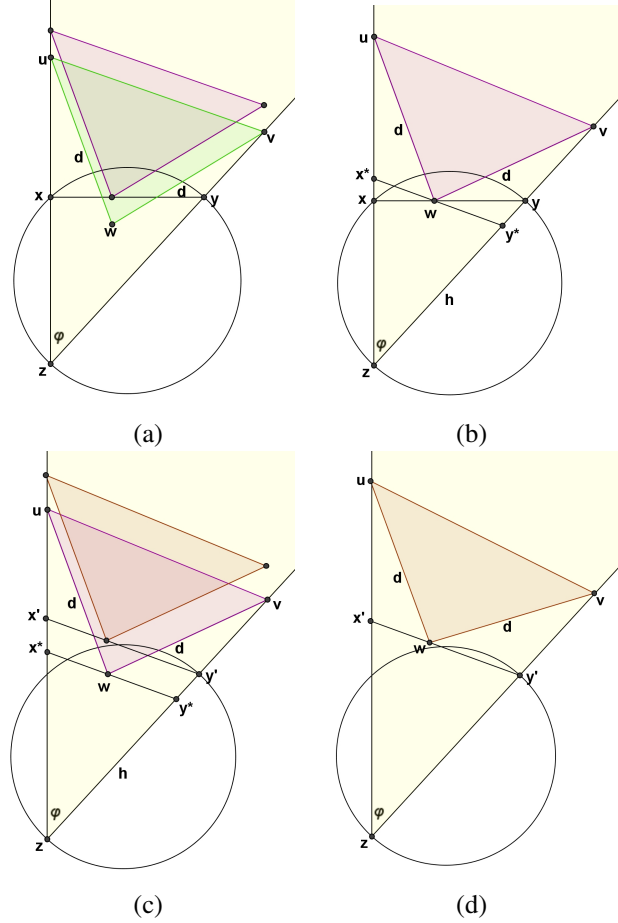


Figure 6. Illustrations for error analysis in Case 1.

Also, $d(x', w) = L' \cdot t$ and $d(w, y') = L' \cdot (1 - t)$, $t \in [0, 1]$. Letting $\angle u w v = \theta(t)$, we have $\theta(t) =$

$$\phi + \arcsin(\sin(\angle u x' y') \frac{L' t}{d}) + \arcsin(\sin(\angle v y' x') \frac{L' (1 - t)}{d}).$$

We have $\frac{\partial \theta}{\partial t} =$

$$\frac{\frac{L'}{d} \sin(\angle u x' y')}{\sqrt{1 - (\sin(\angle u x' y') \frac{L' t}{d})^2}} - \frac{\frac{L'}{d} \sin(\angle v y' x')}{\sqrt{1 - (\sin(\angle v y' x') \frac{L' (1 - t)}{d})^2}}.$$

Setting $\frac{\partial \theta}{\partial t} = 0$,

$$\frac{\frac{L'}{d} \sin(\angle u x' y')}{\sqrt{1 - (\sin(\angle u x' y') \frac{L' t}{d})^2}} = \frac{\frac{L'}{d} \sin(\angle v y' x')}{\sqrt{1 - (\sin(\angle v y' x') \frac{L' (1 - t)}{d})^2}}.$$

Triangle $\triangle x' z y'$ is an isosceles triangle. Therefore, $\angle z x' y' = \angle z y' x'$, $\angle u x' y' = \angle v y' x'$ and hence

$$t^2 = (1 - t)^2,$$

which implies that $t = \frac{1}{2}$. Thus when $t = \frac{1}{2}$, $\theta(t)$ is either a global maximum or a global minimum. We compare the

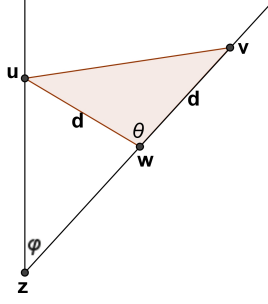


Figure 7. Angle θ is an upper bound for object angle α .

value of $\theta(\frac{1}{2})$ with the values at the extreme points $t = 0, 1$.

$$\begin{aligned}\theta(0) &= \phi + \arcsin\left(\sin(\angle xy'v')\frac{L'}{d}\right), \\ \theta(1) &= \phi + \arcsin\left(\sin(\angle xy'v')\frac{L'}{d}\right), \text{ and} \\ \theta\left(\frac{1}{2}\right) &= \phi + 2 \arcsin\left(\sin(\angle xy'v')\frac{L'}{2d}\right).\end{aligned}$$

As can be shown, $\arcsin(x/2) < \arcsin(x)/2$ for $x > 0$. Since $\angle xy'v' < \pi$, $\sin(\angle xy'v')\frac{L'}{d} > 0$ and hence, $\theta(1/2) < \theta(0) = \theta(1)$. Therefore, $\theta(\frac{1}{2})$ is a global minimum for the function $\theta(t)$ and the maximum occurs when $t = 0$ or $t = 1$.

Thus, the maximum value of $\angle uvw$, θ , is obtained when w is placed at either one of x' or y' . Since $d > L$, the geometry of this configuration is as shown in Figure 7. In particular, $\theta = \phi + \gamma$, where $\phi = \arcsin(\frac{L}{2R})$ and $\gamma = \arcsin(\frac{2R}{d} \sin \phi)$. Thus, $\gamma = \arcsin(\frac{2R}{d} \frac{L}{2R}) = \arcsin(\frac{L}{d})$ and $\theta = \arcsin(\frac{L}{2R}) + \arcsin(\frac{L}{d})$.

The angle $\theta = \angle uvw$ gives an upper bound for the possible value of the object angle α of the missed medial point inside the convex hull of Θ .

Thus, if $d \geq 2L$, object angle $\alpha \leq \theta = \arcsin(\frac{L}{2R}) + \arcsin(\frac{L}{d})$. For a fixed L and R , the value of the object angle α of a missed medial point decreases as d increases. So, if one wants to find medial points with small $d \geq 2L$, one should choose $L \ll d$.

B. Case 2

In this case, we consider the scenario when either $\nabla D(a)$ is to the other side of $l(x, y)$ as $\nabla D(x)$ and $\nabla D(y)$ or $\nabla D(b)$ is to the other side of $l(x', y')$ as $\nabla D(x')$ and $\nabla D(y')$. Without loss of generality, assume that $\nabla D(x)$ and $\nabla D(y)$ are to the other side of $l(x, y)$ as is $\nabla D(a)$. Assume that $l(x, y)$ is oriented horizontally and that $\nabla D(x)$ and $\nabla D(y)$ are above $l(x, y)$, while $\nabla D(a)$ is below.

Let X, Y and P be the nearest points on \mathcal{B} to x, y and p ,

respectively. We know that

$$\begin{aligned}d(x, X) &< d(x, P) \\ d(y, Y) &< d(y, P) \\ d(p, P) &\leq d(p, X) \\ d(p, P) &\leq d(p, Y).\end{aligned}$$

Let $b(a, b)$ be the bisector of points a and b . Then x is above $b(X, P)$ and y is above of $b(Y, P)$, while p can be on or below of $b(X, P)$.

Recall that $d(x, y) \leq L$. Let p' be the point of intersection of (p, P) with (x, y) . We want to know the maximum possible value of $d(p, p')$. We call $d(p, p')$ the *dip* and investigate the relationship between the dip and L .

Let $d = d(p, P)$. When $d < 2L$, this is, arguably a good bound on the quality of the missed medial point.

Consider the case $d \geq 2L$. Suppose that $dip \geq L$ in this case. Since we are in Case 2, $\nabla D(x)$ and $\nabla D(y)$ are to a different side of $l(x, y)$ as is $\nabla D(a)$. We will show that certain conditions must be met when Case 2 holds. To this aim, we will construct an extremal scenario where X and Y are maximally above $l(x, y)$.

Let x^* be the point of intersection of $b(X, P)$ with (x, y) and y^* be the point of intersection of $b(Y, P)$ with (x, y) . To construct a scenario where X and Y are maximally above $l(x, y)$, we want to maximize $\min(\angle xy^*Y, \angle yx^*X)$. This value is largest when $\angle xy^*Y = \angle yx^*X$. Given $b(Y, P)$ and P , point Y is found by dropping a perpendicular from P to $b(Y, P)$ of length l and then traveling distance l in the direction of this perpendicular. Therefore, $\angle xy^*Y$ is largest when the slope of the bisector $b(Y, P)$ is smallest, *i.e.* when $\angle py^*x$ is smallest. A lower bound on the slope of $b(Y, P)$ is achieved by aligning it with p and y . Similarly, we achieve a lower bound on the slope of $b(X, P)$ by aligning $b(X, P)$ with x and p . Since $\angle xy^*Y = \angle yx^*X$, $b(X, P)$ and $b(Y, P)$ have the same slope, *i.e.*, $\angle pxy = \angle pyx$. This implies that $d(x, p) = d(p, y)$. Refer to Figure 8. Let b_{XP} be the intersection of $b(X, P)$ with $l(X, P)$. Define

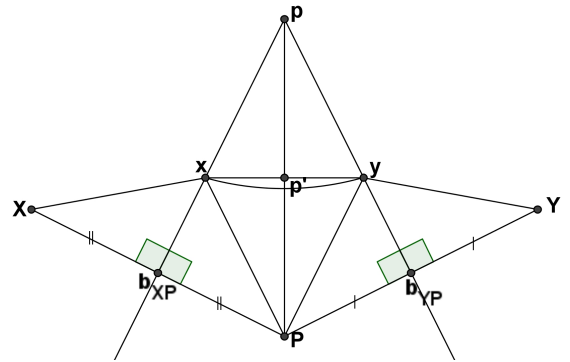


Figure 8. The angles of interest in Case 2.

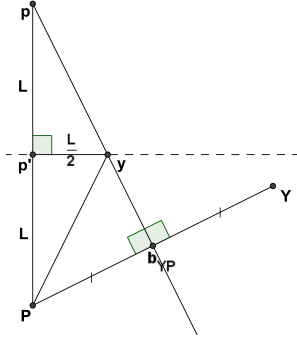


Figure 9. When (p, P) is orthogonal to (x, y) and $dip \geq L$, $d \geq 2L$, the y -coordinate of Y is $\approx -0.21L$.

b_{YP} similarly. By construction, $\angle Xxb_{XP} = \angle b_{XP}xP$ and also $\angle Pyb_{YP} = \angle b_{YP}yY$. Since $\angle xyY = \angle yxX$, $2\angle b_{XP}xP + \angle Pxy = 2\angle b_{YP}yY + \angle Pyx$. Combining this with the fact that $\angle b_{XP}xP + \angle Pxy = \angle b_{YP}yY + \angle Pyx$, we get that $\angle b_{XP}xP = \angle b_{YP}yY$. Hence $\angle Pxy = \angle Pyx$ and $d(P, y) = d(P, x)$. Since $d(P, y) = d(P, x)$ and $d(x, p) = d(y, p)$, the quadrilateral $xpyP$ has the property that its diagonals (x, y) and (p, P) intersect at right angles. Their point of intersection is p' and $d(x, p') = d(p', y)$.

An upper bound for $d(x, p') = d(p', y)$ is $L/2$. Setting $d(x, p') = d(p', y)$ to the largest possible value $L/2$ makes the slope of $b(Y, P)$ smallest. By the arguments in the previous paragraph, when the slope of $b(Y, P)$ is smallest, segment (p, p') is orthogonal to (x, y) and $b(Y, P)$ passes through p and y . Now suppose that $d = d(p, P) = 2L$, $dip = d(p, p') = L$ and (x, y) is aligned with the horizontal, as shown in Figure 9. In this case, the y -coordinate of Y is $\approx -0.21L$ and so, $\nabla D(y)$ lies to the same side of (x, y) as $\nabla D(a)$. Since we have considered the highest possible placement of Y , it is not possible that $d = 2L$ and $dip = L$. Further, for $d \geq 2L$ and $d(p', P) \geq L$, Y remains below $l(x, y)$.

Therefore, when $d \geq 2L$ and $d(p', P) \geq L$, $dip < L$. So, in summary for case 2, either $dip < L$ or $d < 2L$ or $d(p', P) < L$. In the future, when we say that medial point p has nearest points on \mathcal{B} near C , we mean that $d(p', P)$ is small.

C. Error Bound

In our discussion of the error in cases 1 and 2, we have proven the following theorem:

Theorem 10: Let $\mathcal{B} \subset \mathbb{R}^2$ and C be a circle that does not contain in its interior any part of \mathcal{B} . Let Φ be a set of sample points on C . Suppose that $\text{DECIDEMA2D}(\mathcal{B}, C, \Phi)$ returns ‘Undetermined’, yet a medial point p is inside the convex hull of $\Theta = \Phi \cup \{\text{opp}(\phi_i) \mid \phi_i \in \Phi\}$. Let L be the maximum shortest arc length between two neighbouring sample points in Θ and let R be the radius of the circle C . Let two of

the nearest points on \mathcal{B} to p be A and B . Let $d = d(p, A)$, $\alpha = \angle ApB$, a' be the point of intersection of (p, A) with the convex hull of Θ , b' be the point of intersection of (p, B) with the convex hull of Θ .

If $L < 2R$, then either

- 1) $d < 2L$,
- 2) $\alpha \leq \arcsin(\frac{L}{2R}) + \arcsin(\frac{L}{d})$,
- 3) $d(p, a') < L$,
- 4) $d(p, b') < L$,
- 5) $d(a', A) < L$, or
- 6) $d(b', B) < L$.

Therefore, when L is small, a missed medial point will either have small distance to the boundary, small object angle, small dip or will have nearest points on \mathcal{B} near C . In the next section, we shall evaluate the significance of these error measures and also show how algorithm DECIDEMA2D can be used to build an algorithm for the detection of a dense collection of medial points with bounded error.

VI. MEDIAL AXIS APPROXIMATION

Small perturbations of \mathcal{B} can result in significant perturbations of its medial axis M . For this reason, it is common to approximate the medial axis M using a stable subset of medial points. Popular simplification schemes favour medial points with large object angle α [1], [2], [9], [14], [13] and large distance d to \mathcal{B} [1], [16]. Thus, object angle and distance to \mathcal{B} of any missed medial points are reasonable quantities to bound when evaluating quality of Algorithm DECIDEMA2D .

In order to use DECIDEMA2D to find a dense sampling of medial points on the medial axis, we cover $\mathbb{R}^2 \setminus \mathcal{B}$ with overlapping circles of varying radii. By using overlapping circles, we ensure that if a medial point has a shallow dip in one circle, it will have a bigger dip in a neighbouring circle. Recall that when the circle C is near \mathcal{B} , it is possible that DECIDEMA2D fails to detect medial points in C . We overcome this limitation by using circles of varying radii. If we place small circles near \mathcal{B} and if medial points fail to be detected in these, then such medial points will have small d and will be candidates for pruning. Therefore, the medial points found by covering space with overlapping circles of varying radii are ones that have either a small object angle or small distance to the boundary. Thus, it is possible to design a distance field method that, in 2D, provably detects those regions of space that contain medial points of large object angle and large distance to the boundary.

Finally, to locate medial points inside a circle C that is chosen by Algorithm DECIDEMA2D as containing medial points, we can perform binary search along appropriate line segments (θ_i, θ_j) , where $\theta_i, \theta_j \in \Theta$, to find the approximate location where a ∇D vector changes direction or crosses a line between two sampled points. We can choose to retain only those medial points that satisfy a user-specified thresh-

old for object angle and distance to the boundary. Let us call the algorithm we have just described APPROXMA2D.

VII. EXPERIMENTAL RESULTS

Encouraged by the results of the 2D analysis, which showed that the medial points that are missed by algorithm DECIDEMA2D are of little interest, we extend DECIDEMA2D for use in a 3D algorithm DECIDEMA3D (see Algorithm 2). Since the conclusions of Lemma 4 hold in 3D as well, the correctness of DecideMA3D follows. We use DECIDEMA3D to build algorithm APPROXMA3D that returns a set \mathcal{M} of medial points and has 3 user-specified parameters: distance of points in \mathcal{M} to the medial axis ϵ , density of \mathcal{M} , and object angle threshold α . APPROXMA3D tiles space with cubes of a coarse resolution. These cubes are then circumscribed with spheres. Those cubes whose circumscribing spheres are believed to contain medial points are subdivided, and the process is repeated until we reach the desired resolution. Then one medial point is found per cube that is within ϵ of the medial axis using binary search along line segments (θ_i, θ_j) for all the queried points Θ on S . We retain those medial points that have an object angle above α . The result is a densely sampled medial axis, where the density is user-prescribed. We have implemented this method and some outputs are shown in Figure 10. Note that since the exact computation of the medial axis for polyhedra with such a large number of faces (tens of thousands) is not feasible, ground truth medial axes are not available for comparison in this case.

Although a theoretical analysis of our 3D algorithm remains as future work, the analysis in this article for the 2D case, as well as the quality of our experimental findings for 3D, as assessed by visual inspection, suggest that the extension of algorithm ApproxMA2D to 3D is well justified.

A. Voronoi diagram of a set of disjoint sites

To illustrate that our method can be made to work with arbitrary inputs \mathcal{B} , we also show the Voronoi diagram of 3 lines computed with our method in Figure 11. Note that algorithms DECIDEMA2D and DECIDEMA3D remain correct for any choice of boundary \mathcal{B} . Given a fast way to compute distances from points to \mathcal{B} , it is possible to use our method to compute medial axes for any variety of disjoint sites, including polygons, curves, circles, spheres, polyhedra. When the sites are convex, the medial axis corresponds to the Voronoi diagram of the objects. Otherwise, pruning of portions of the medial axis produces the Voronoi diagram.

VIII. CONCLUSIONS

We have presented the first, to our knowledge, analysis of the relationship between the number and distribution of query points and the quality of the approximation for a distance field method for medial axis approximation in 2D. This analysis is an indication that distance field methods

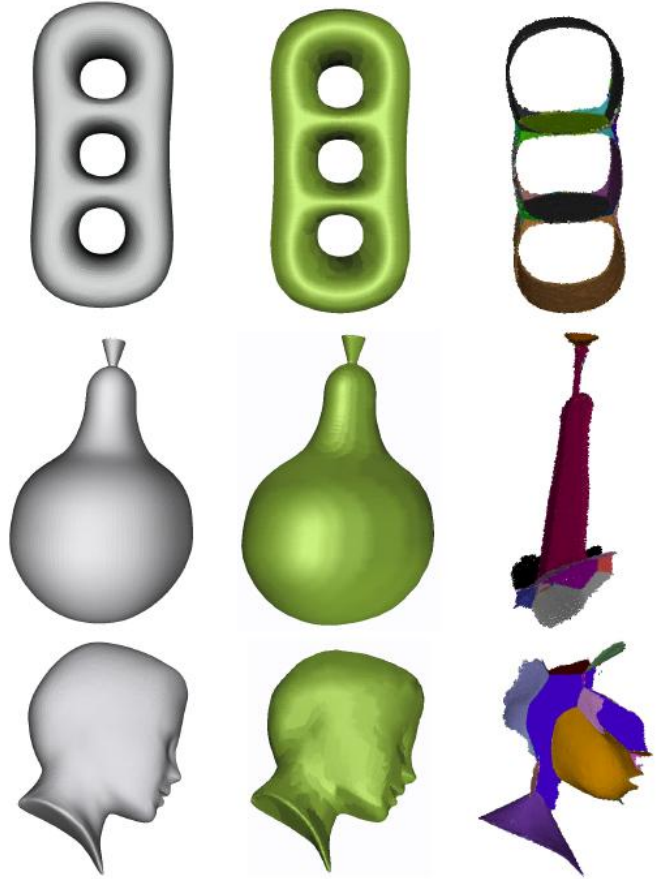


Figure 10. The original polyhedra (left), their medial axes (right) and the reconstruction of the original object as the union of medial spheres (centre).

Algorithm 2 DECIDEMA3D(\mathcal{B}, S, Φ)

Require: Boundary \mathcal{B} , sphere S not intersecting \mathcal{B} , set of points Φ distributed on S .

Ensure: ‘True’ if S contains a medial point, ‘Undetermined’ if no such conclusion can be drawn.

- 1: **for all** $\phi_i \in \Phi$ **do**
 - 2: **if** $\nabla D(\phi_i) \neq \nabla D(\text{opp}(\phi_i))$ **then**
 - 3: Return ‘True’
 - 4: **end if**
 - 5: **end for**
 - 6: Return ‘Undetermined’
-

have the potential to provide medial axis approximations that are consistent with accepted quality measures in terms of object angle and distance from medial points to the boundary.

We have presented experimental results for a 3D version of our method, showing medial axes of polyhedral and line segment inputs. Our results suggest that a similar relationship exists between number of sample points and quality of approximation for the 3D case.

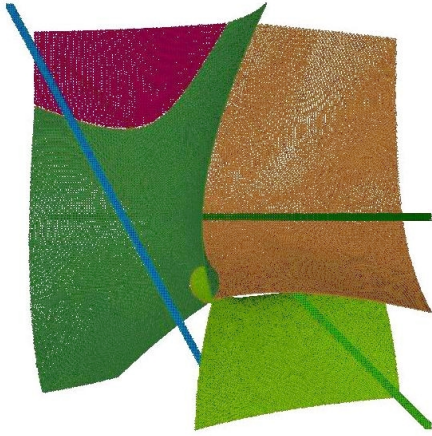


Figure 11. Voronoi diagram of 3 lines cropped to a cube.

ACKNOWLEDGMENT

We would like to thank Kaleem Siddiqi for encouraging this work and suggesting reference [15]. We are grateful to financial support from NSERC Canada and FQRNT Québec.

REFERENCES

- [1] N. Amenta, S. Choi, and R. Kolluri, "The Power Crust, Unions of Balls, and the Medial Axis Transform," *Computational Geometry: Theory and Applications*, vol. 19, no. 2-3, pp. 127–153, 2001.
- [2] T. K. Dey and W. Zhao, "Approximating the medial axis from the Voronoi diagram with a convergence guarantee," *Algorithmica*, vol. 38, pp. 387–398, 2004.
- [3] F. Chin, J. Snoeyink, and C. A. Wang, "Finding the medial axis of a simple polygon in linear time," in *International Symposium on Algorithms and Computation*. Springer-Verlag, 1995, pp. 382–391.
- [4] H. Blum, "Biological Shape and Visual Science," *Journal of Theoretical Biology*, vol. 38, pp. 205–287, 1973.
- [5] S. Yoshizawa, A. Belyaev, and H.-P. Seidel, "Skeleton-based variational mesh deformations," *Computer Graphics Forum (Proc. EUROGRAPHICS)*, vol. 26, no. 3, pp. 255–264, September 2007.
- [6] S. Bouix, K. Siddiqi, and A. Tannenbaum, "Flux driven automatic centerline extraction," *Medical Image Analysis*, vol. 9, no. 3, pp. 209–221, 2005.
- [7] K. Siddiqi, J. Zhang, D. Macrini, A. Shokoufandeh, S. Bouix, and S. Dickinson, "Retrieving articulated 3-d models using medial surfaces," *Machine Vision and Applications*, vol. 19, no. 4, pp. 261–275, 2008.
- [8] K. Siddiqi and S. Pizer, Eds., *Medial representations: mathematics, algorithms and applications*. Springer, 2008.
- [9] P. Dimitrov, J. N. Damon, and K. Siddiqi, "Flux invariants for shape," in *Computer Vision and Pattern Recognition*, 2003, pp. 835–841.
- [10] T. Culver, J. Keyser, and D. Manocha, "Exact computation of the medial axis of a polyhedron," *Computer Aided Geometric Design*, vol. 21, no. 1, pp. 65–98, 2004.
- [11] J. M. Vleugels and M. H. Overmars, "Approximating generalized voronoi diagrams in any dimension," Department of Information and Computing Sciences, Utrecht University, Tech. Rep. UU-CS-1995-14, 1995.
- [12] M. Etzion and A. Rappoport, "Computing voronoi skeletons of a 3-d polyhedron by space subdivision," *Computational Geometry: Theory and Applications*, vol. 21, pp. 87–120, 2002.
- [13] M. Foskey, M. C. Lin, and D. Manocha, "Efficient computation of a simplified medial axis," in *Solid modeling and applications*, 2003, pp. 96–107.
- [14] S. Stolpner and K. Siddiqi, "Revealing significant medial structure in polyhedral meshes," in *3D Data Processing, Visualization, and Transmission*, 2006, pp. 365–372.
- [15] B. Kimia, A. Tannenbaum, and S. Zucker, "On the evolution of curves via a function of curvature. I: The classical case," *Journal of Mathematical Analysis and Applications*, vol. 163, pp. 438–458, 1992.
- [16] F. Chazal and A. Lieutier, "The λ -medial axis," *Graphical Models*, vol. 67, no. 4, pp. 304–331, 2005.